Separating Local and Propagated Contributors to the Behnke-fried Microelectrode Recordings

P. Jurczynski[1], S. Le Cam[1], B. Rossion[1,2] and R. Ranta[1]

[1]*Université de Lorraine, CNRS, CRAN, F-54000 Nancy, France*
[2]*Université de Lorraine, CHRU-Nancy, Service de Neurologie, F-54000, France*

Keywords: Microelectrode, Local Field Potential, Reference Estimation, Zero-reference Montage.

Abstract: In electrophysiological measurements, a recording electrode is located in an electric field and has a certain electric potential value. Each measured signal is a potential difference between two electrodes, a measuring electrode and a so-called reference electrode. This reference electrode is not located at infinity and outside of any electric field, thus its electric potential is found in the measured signals. In order to isolate the local activity of the recorded structure, it is necessary to understand the relationships between the different contributors at the electrode level and separate these different activities. In this paper, we focus on the particular setup of Behnke-Fried micro-electrodes. We propose to adapt a previous re-referencing method for separating local and distant propagated activities taking into account the non-stationarity of the signals and the particular geometry of these microelectrodes. We demonstrate, on realistically simulated signals, that the new re-referencing procedure improves the preprocessing of these signals and might help deeper interpretation.

1 INTRODUCTION

Microelectrode recordings make it possible to analyze the activity of the very close neuronal population in which the electrode is implanted, within a radius of a few hundred micrometers depending on the type of implanted microelectrode. Such measurements have been widely used to analyze the activity of individual neurons, the action potentials (AP) of close neurons being one of the main contributors to the recorded signal. A second main contributor to the signal are the inhibitory and excitatory post-synaptic currents, which mainly originate from the local population, but can also be picked from more distant structures up to several millimeters if their activities are synchronized enough (Buzsáki et al., 2012; Kajikawa and Schroeder, 2011). The analysis of these dominant contributors and of their relationships hold precious information to interpret the activity of the implanted structure (Einevoll et al., 2013), their separations being a prerequisite to such analysis.

This separation, which is already a challenging signal processing task by itself due to overlaps between their (frequency) contents (Zanos et al., 2011), is made even more complicated by the presence of the reference potential. Indeed, the measured electrical activity always corresponds to a potential dif-

ference - one electrode measures the potential relative to another electrode, considered as the reference. The relationship between the potentials "seen" by the reference electrode and by the measuring electrodes depend on the particular recording setup. For example, in the context of macroscopic EEG recordings, the reference is often one of the scalp electrodes, fundamentally similar to the other (measuring) scalp electrodes. In the intracerebral recordings context (SEEG), the reference is either considered to be at zero potential, or at least sufficiently far away from the other electrodes so that the reference potential can be considered independent (or at least uncorrelated) with respect to the potential of interest (Libenson, 2012; Yao, 2001; Hu et al., 2007).

By the fact that all signals are potential differences between measuring and reference electrodes, the potential of the latter is implicitly present in all signals to be analyzed. This is also the case for microelectrodes recordings, and in particular for Behnke-Fried electrodes, which are the focus of this work. These electrodes (manufactured by AdTech and one of the few microelectrode devices certified for human brain invasive recordings), are mixed macro-micro electrodes, with nine micro-wires deployed in the brain at the tip of a SEEG macro electrode, one of them being chosen as the reference electrode (see figure 1).
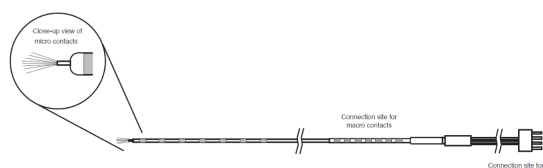
Figure 1: Behnke-Fried electrode. Image from AdTech website.

In all cases, the reference signal can be seen as "perturbation" which does not hold information on the local activity of interest generated around the measuring electrodes, and several methods have been developed for its cancelling. One of the simplest techniques is the bipolar montage, which subtracts two signals one from the other, achieving for one hand at reference cancelling and, for the other hand yielding an estimate of the local activity originated between and around the two involved electrodes. While in theory possible for Behnke-Fried recordings, the interpretation of such a montage is difficult, because it is impossible to know the microelectrodes respective positions exactly. Indeed, the microelectrodes are at the and of flexible microwires, not visible on CT scan as in the case of SEEG macroelectrodes (Hofmanis et al., 2011). The same reasoning holds for Laplacian / CSD estimates of local sources (Mitzdorf, 1985; Hjorth, 1975). Moreover, because the positions are not known, a forward-inverse model based solution like REST (Yao, 2001; Salido-Ruiz et al., 2019) is not possible neither.

Two other solutions are proposed in the literature: the average reference (*i.e* estimating the reference potential by averaging all measured signals and subtracting it from them) and a weighted average reference estimation. The first contribution belonging to this last family of solutions was the PCA-based blind source separation proposed in (Hu et al., 2008), further developed and justified for the elimination of the SEEG reference by (Ranta et al., 2010). This solution, called "zero-reference" (ZR) by the authors, has been shown to be equivalent to the minimum power distortionless response beamformer (MPDR), well known in array signal processing, and which also maximises the signal-to-noise ratio (SNR) (Madhu et al., 2012).

The first objective of this paper is to demonstrate that this zero-reference method can make an important contribution to the separation of components in the context of Behnke Fried electrode recordings. The solution depends on the quality of the estimation of some statistical measures from the data (covariance matrix), which are difficult to estimate in the context of non-stationary signals. To cope with this problem, we also propose in this paper an adaptative version of this zero-reference algorithm.

The paper is organized as follows: first we introduce the existing re-referencing methods in the context. We next present the zero-reference method and its update to make it adaptive over time. Finally, these common activity estimation methods (average, ZR, adaptive ZR) will be evaluated on simulated and real data. In particular, it will be shown that this treatment enhance the robustness of AP detection, which is very often an important prerequisite to spike sorting algorithms. Also its importance for further spike to LFP relationship will be illustrated in the context of Fast Periodic Visual Stimulation (FPVS) simulated data. Finally, to the extent that propagated distant activities can also be seen as external perturbations, re-referencing becomes an artifact reduction technique. An example of such artifact reduction and of its effects on spike analysis is presented on real microelectrode signals.

2 COMMON ACTIVITY ESTIMATION

2.1 Model

In any point inside the brain, the extracellular potentials are a mixture due to close and far current sources of different natures: synchronized synaptic potentials seen far from their originating point (like in the EEG case), local synaptic activities due to the local population, more or less synchronized, and extracellular action potentials, due to very close neurons. Issued from different biophysical phenomena, these activities have different time-frequency characteristics, although partially overlapping (Zanos et al., 2011).

The way we see them depends on the measuring setup. We will not enter here in the detailed modelling of the electrodes physics (see *e.g* (Nelson et al., 2008)), but we will consider an approximate model of the electrodes that interest us (Behnke-Fried). As mentioned, they consist of nine microwires deployed at the tip of an intracerebral macroelectrode. One of the nine microwires is used as a reference electrode. But this electrode has the specificity to be stripped from its insulation on several millimeters at its extremity, while the 8 others are not. The former is then exposed to the brain electrical field on a larger surface ($\approx 1mm^2$) compared to the latter, with a much smaller recording surface ($\approx 3000\mu m^2$), then a surface ratio of the order of two to three magnitude. Consequently, the nature of the activity captured on the reference electrode is different with respect to the much more local potentials acquired by the 8 remain-

ing microwires. Indeed, due to averaging effect over a larger surface (Hagen et al., 2016), the activities due to very local structure such as individual neurons (AP) and group of neurons (local LFP) are drastically diminished. On the other hand, the reference electrode itself is not at zero potential, but picks up an average activity of the surrounding brain structures with sufficient synchronization, such as suggested in (Lindén et al., 2010). Although the other 8 measuring microelectrodes are under the influence of the same propagated electrical field originating from distant brain sources, their impedance is higher thus the amplitude of the propagated potential is not the same as the one captured by the reference electrode. To sum up, every available signal x_i ($i = 1..8$) can be written as:

$$x_i = x_{local} + \alpha x_{distant} - x_{distant} \tag{1}$$

with x_{local} a mixture of extracellular action potentials and local synaptic activity and $x_{distant}$ the propagated synaptic activity of far sources captured by the reference electrode ($x_{distant} = r$, α standing for the different gain that the distant activity has on the measuring electrodes with respect to the reference electrode). As the actual amplitude of the propagated $x_{distant}$ is unknown, equation (1) can also be written as:

$$x_i = x_{local} - r \tag{2}$$

or, in matrix form,

$$\mathbf{x} = \begin{bmatrix} \mathbf{A} & \begin{matrix} -1 \\ \vdots \\ -1 \end{matrix} \end{bmatrix} \begin{bmatrix} \mathbf{s} \\ r \end{bmatrix} \tag{3}$$

where $\mathbf{x} \in \mathbb{R}^{(M \times 1)}$ is the vector of measured signals ($M = 8$ in our case), $\mathbf{A}$ is some mixing matrix accounting for possible correlations between the local activities, $\mathbf{s}$ are a basis for the local signal space (local neural sources) and r the reference potential equal to a scaled version of the propagated activities $x_{distant}$. In other words, it should be possible to use reference cancelling techniques for separating between local and propagated components of the recorded signals.

2.2 State of Art

As noted in the Introduction, several techniques already exist to eliminate common reference activity, depending on the measuring setup. Biophysically founded methods such as REST or Laplacian/CSD (common in EEG but not only), are not adapted for the Behnke-Fried electrodes because the position are unknown. One of the simplest remaining solutions is the average reference estimation, which approximates r as the average of x_i.

More elaborated methods were developed for the SEEG setup, for which the basic hypothesis is that the reference potential is uncorrelated with the potentials of the measuring electrodes. This hypothesis holds also for the application we study here. Indeed, the so-called local activities x_{local} are a sum of action potentials and local synaptic potentials. If it is very unlikely to have correlated spike trains between two electrodes, it could be in principle possible to have correlated synaptic activities. But in all cases, we can rather safely make the hypothesis that these local activities are not correlated with the activity of distant synchronized populations $x_{distant}$ and thus to the reference potential r.

The zero-reference method was introduced in a series of papers starting with (Ranta et al., 2010), which propose to improve previous methods developed by *e.g* (Hu et al., 2007). It is based on a semi-blind source separation / beamforming technique. The basic assumption is that the potential of the common reference electrode is decorrelated from the potentials of the measuring electrodes.

Under the decorrelation hypothesis, one can show that the best estimate (Madhu et al., 2012) (in a minimum squares error sense) of the reference potential (which has to be added to $\mathbf{x}$ for re-referencing) is:

$$\hat{r} = \mathbf{w}^T \mathbf{x}, \quad \text{with} \quad \mathbf{w} = \frac{\mathbf{R_{xx}}^{-1}}{\mathbf{1}^T \mathbf{R_{xx}}^{-1} \mathbf{1}} \mathbf{1} \tag{4}$$

where $\mathbf{R_{xx}}$ is the covariance matrix of the measured signals $\mathbf{x}$ and $\mathbf{1}$ is a vector of ones.

2.3 Adaptive RLS Method

The zero-reference method seen above is implicitly based on the assumption that the signals are stationary and thus the correlation matrix does not vary over time. However, a stationary model is not accurate when processing brain signals. In order to improve the method, we propose to make it adaptive by estimating the covariance matrix at every time step, using the well known exponentially weighted Recursive Least Squares (RLS) signal processing algorithm (Eleftheriou and Falconer, 1986).

This method makes it possible to calculate iteratively the inverse of the covariance matrix $\mathbf{R_{xx}}$ (see eq. 4) at time $t + 1$ thanks to the inverse covariance matrix at time t:

$$\mathbf{R_{xx}}(t+1)^{-1} = \lambda^{-1}(\mathbf{R_{xx}}(t)^{-1} - \mathbf{G}(t+1)\mathbf{R_{xx}}(t)^{-1}) \tag{5}$$

with

$$\mathbf{G}(t+1) = \frac{\lambda^{-1}\mathbf{R_{xx}}(t)^{-1}\mathbf{x}(t+1)\mathbf{x}^T(t+1)}{1 + \lambda^{-1}\mathbf{x}^T(t+1)\mathbf{R_{xx}}(t)^{-1}\mathbf{x}(t+1)} \tag{6}$$

where $\mathbf{x}(t)$ is the $M \times 1$ vector of the measured signals at instant t, $\mathbf{R_{xx}}(t)$ is the covariance matrix at instant t, λ is the forgetting factor and $\mathbf{G}(t+1)$ an update factor including the well-known Kalman gain.

The adaptive estimation of the common potential r present on the $M = 8$ electrodes (3) will then be performed at each time step by replacing $\mathbf{R_{xx}}$ in (4) by its adaptive estimate given by (5) and (6).

3 RESULTS

3.1 Simulations

We use simulated data to compare the respective performances of the average montage, the adaptive and the non-adaptive zero referencing methods. 8 non stationary (two concatenated stationary epochs) correlated signals are simulated by reproducing realistic frequencies as observed in real electrophysiology (typical theta and gamma physiological brain rhythms), representing the local potential activities as seen by the 8 microelectrodes (Figure 2, second row). On one signal, a specific LFP with frequency 1.2Hz is added, simulating the synaptic response to a specific stimuli (e.g. a visual stimuli (Rossion et al., 2020)), on which a synchronized train of simulated action potentials (Tran et al., 2020) are superimposed following a Poisson distribution with a 1.2Hz varying firing rate (Figure 2, first row). On 4 of the 7 remaining signals, action potentials are also randomly added, while the 2 others are left free of spikes. A ninth signal is simulated, having a power spectral density reproducing the one observed on raw micro recordings, representing the propagated distant LFP ($x_{distant}$ in (1)) as picked up by the reference electrode. Although mainly lying in the lower frequency band (below $100Hz$), this signal contains significant frequency components up to $350Hz$, thus partly recovering the frequency components of the action potentials (Figure 2, third row). This synthetic reference potential is simulated uncorrelated with the first 8 signals representing local measuring microelectrode potentials (x_{local} in (1)), to be in line with the prerequisite of the zero-reference montage. The former are substracted to the latter to build the simulated microelectrode recordings x (Figure 2, last row). Finally, random Gaussian noise is added on the 8 channels, with a signal to noise ratio SNR=4.

3.2 Reference Signal Estimation

In order to compare the adaptive method with the non-adaptive one and to the average montage, 50 realizations of simulated sets of signals as described above have been carried out. The performance criterion is the correlation of the simulated reference with the estimated reference, calculated for each methods. From the boxplots of figure 3, we can see that the correlation score are significantly higher when using the adaptive method compared to the two other approaches, the average montage showing the worst performance. The figure 4 illustrates the ability of the adaptive method in estimating the reference signal, visually superior to the ones given by the non-adaptive as well as the average methods.

3.3 Re-referencing for Spike Detection

The detection of spikes is a pre-requisite to the analysis of the spiking activity of neurons located around the electrode. This challenging task, if not carried out with enough care, can lead to misinterpretation regarding the role of the implanted structure. Removing the reference that has frequencies straddling the spikes should improve their detection, as well as their classification. In this paper, we focus on the influence of the re-referencing on the accuracy of the detection task. We consider here the classical method of detection consisting in a bandpass filter between 300 Hz and 6000 Hz that removes low frequencies commonly attributed to the LFP. Then, a threshold calculation depending on the MAD (Median absolute deviation) is used to detect the action potential peaks on the signal (Quian Quiroga et al., 2004).

As described above, trains of simulated spikes have been added on 5 of the 8 microelectrode channels. Several simulations were performed, with different spike amplitudes and thus different spike to LFP ratios (seen as SNR). These amplitudes have been fixed to reach peaks-to-noise ratio, defined as the maximum amplitude of the spike divided by the standard-deviation of the raw microelectrode signal, in the range 3 to 7.

We compare the result of the detection on the raw data and on the re-referenced data with the adaptive zero-referencing method (for this task, no significant difference are reported between the adaptive and no-adaptive method). Bar graphs of Figure 5 provide a summary of the detection results, namely the percentage of spikes detected with and without re-referencing, for different amplitudes of the spike to be detected (different SNRs). It should be noted that the number of false positives is less than 1% of the spikes detected in all the simulations, so it will be neglected in this study. The percentage of spikes detected is consistently higher on the zero-referenced signal than on the raw signal, whatever the amplitude of the peaks. Clearly, the smaller the amplitude of the
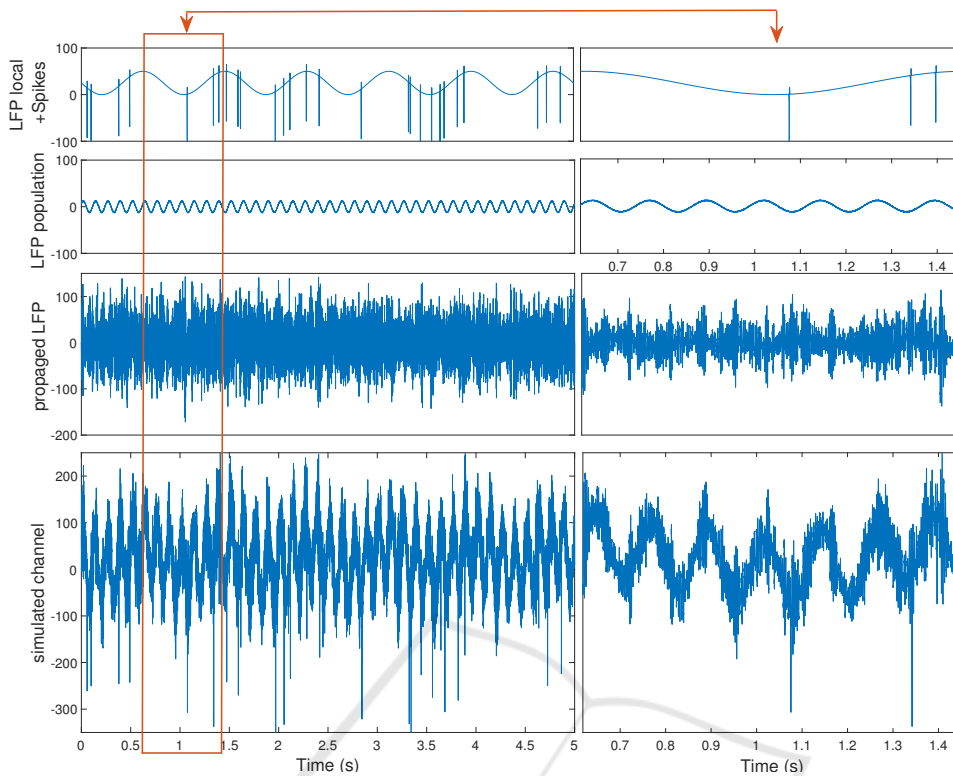
Figure 2: Example of simulated channel and its components (with a zoom in the right panel). First row : 1.2Hz response to the stimuli superimposed with a synchronized spike train (one can see bursts of spikes locked to the same phase of the response). Second row : other local LFP as seen by the microelectrode (correlated with the other channels). The sum of the first two rows yields the local activity x_{local} in (1). Third line : propagated LFP as seen by the reference electrode ($r = x_{distant}$). The last row is the resulting simulated microelectrode recording x obtained as a combination of the first three rows.
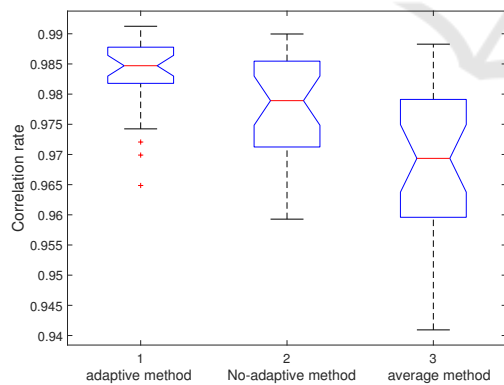

Figure 3: Correlation coefficients between the simulated reference and the estimated ones using the adaptive RLS method (1), the classical ZR method (2) and the average reference (3), over 50 simulations.

peaks is in relation to the background LFP, the greater the influence of the re-referencing for spike detection will be. When the peak-to-noise ratio fall to 3, only about 10% of the spikes are detected on the raw signal, while more than 60% of them are recovered on the re-referenced signal. This emphasizes the impor-

tance of extracting the local activity from the propagated (reference) signal for accurate spike detection, in particular for detecting spikes with low amplitudes, i.e. those originating from neurons that are not in the very close vicinity of the electrode. The impact of the re-referencing on the accuracy of spike sorting algorithm might also be significant, by eliminating the overlapping components of the reference signal in the high frequency band over $300Hz$ and delivering a better estimation of the spike shapes. This will be evaluated in future works.

3.4 Spikes and LFP Synchronisation

The starting point for this section is the study of face recognition mechanisms in humans with fast periodic visual stimulation (FPVS). In one of the key FPVS paradigms, natural variable photographs of faces are presented at a frequency of 1.2 Hz among images showing various living and non-living objects at 6 Hz (Rossion et al., 2015). This stimulation leads a generic neural response in the visual cortex at 6Hz, and a response at 1.2 Hz from populations of neurons responding selectivity (i.e. differentially) to faces.
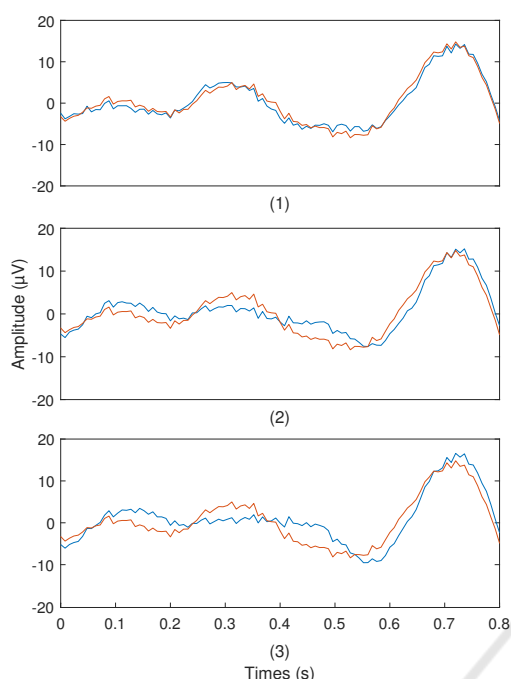
Figure 4: Simulated reference (orange) and estimated reference (blue) using the adaptive RLS method (1), the ZR method (2) and average (3).
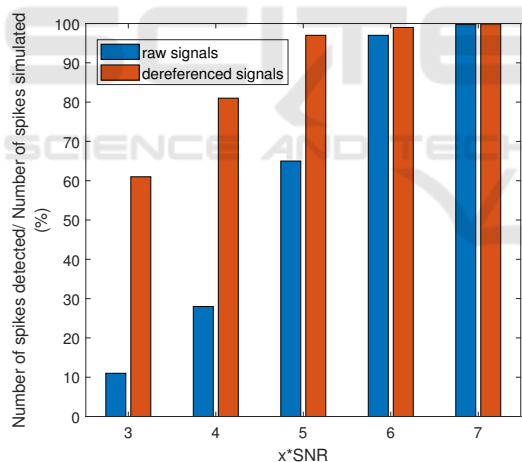

Figure 5: Percent of spike detected on raw signal (blue) and re-referenced signal (orange).

When recording from a face-selective cortical region such as the lateral middle fusiform gyrus, it is thus likely that local neural activity is expressed 1.2 Hz while distant-neural activity at 6 Hz is mainly captured by the reference electrode.

Eliminating the reference signal from the microelectrode recordings provides a more local vision of the neural activity (synaptic LFP+spikes) surrounding each microelectrode, therefore not corrupted anymore by remote neural activity unlikely to be related to the local spiking activity. This procedure will help

in evaluating the synchrony between the local LFP and the spiking activity, or a consistent response of the LFP with respect to a given stimuli. The aim of this section is to illustrate that the activity of the propagated LFP (seen here as the reference) contaminates the local LFP as seen by a given electrode, and can mask or make it difficult to identify such relations.

To do this, we consider the microelectrode signal on which a 1.2Hz face-selectivity response has been simulated. From stimulus onset, windows of 200 milliseconds succeeding each trigger can be selected and averaged, and an average LFP pattern (evoked potential), synchronized with the stimuli, should emerge.

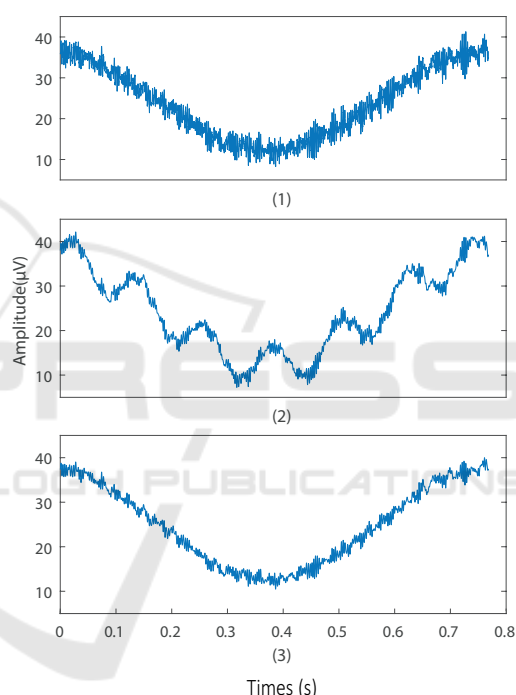It is immediately noticeable in Figure 6 that a

Figure 6: Local simulated LFP (1), raw simulated LFP (2) and re-referenced LFP (3) (same time window as the right panel in figure 2).

parasitic frequency appears when such stimuli triggered averaging is applied on the raw signal. This 6Hz activity originating from the propagated LFP (reference), is a multiple of the 1.2Hz stimulation frequency, disturbing the identification of the local pattern. Once the reference is removed, this frequency no longer appears and the resulting signal is very close to the expected one.

3.5 Observations on Real Data

In this section, we evaluate the re-referencing results on a 2 minutes long window taken from a Behnke-

Fried micro-electrodes recordings, containing 8 channels sampled at 32kHz, and recorded in the anterior human hippocampus of an epileptic patient. The effect of the re-referencing was evaluated in terms of artifact reduction, without altering the information contained in the signals (spikes / LFP).
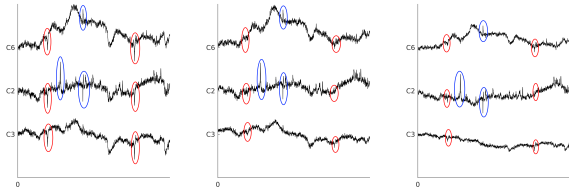

Figure 7: Example of re-referencing. Left: raw (common reference) signals, Middle: zero-referenced signals, Right: average-referenced signals. Artifacts are circled in red, spikes in blue.

Figure 7 presents 130ms of recording on 3 channels. Artifacts are circled in red (they are considered artifacts because they are present on all the channels and have a distinct shape from a spike). Referencing by zero reference and average reference eliminates these artifacts, without removing the neural spikes (circled in blue). However, it can be noted that the average distorts the low frequency activity of the signal (right-most panel, figure 7), which is not the case with the zero-reference. Moreover, the spike shapes (obtained here after applying a home-made Bayesian spike sorting / despiking alogorithm (Le Cam et al., 2019) inspired from (Zanos et al., 2011)) are preserved by the zero-referencing method while they are distorted by the average referencing (Figure 8, right-most respectively middle panels).
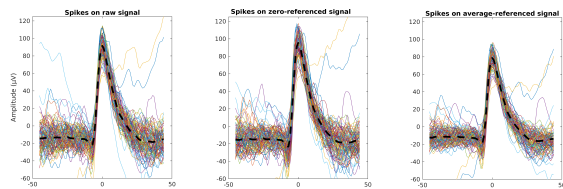

Figure 8: Superimposed spikes from a single unit (same order as above).

Re-referencing has very little effect on spike sorting except for the removal of artifacts common to several channels. The objective of re-referencing is more focused on the separation of low frequency components in order to optimize the study of relationships.

4 CONCLUSION

The separation of components in the particular case of Behnke-Fried microelectrodes is important for an-

alyzing the activity of the implanted region, in particular for understanding the relationships between the different contributors to these recordings. We develop in this paper an adaptative reference estimation method which allows a separation of the local activity close to the electrodes, consisting in spikes and local LFP, from a propagated LFP activity originating from distant structures.

The use of such re-referencing as a pre-processing to microelectrode signals allows a better analysis of the very local activity around each microelectrode, consisting of local LFP as well as the spiking activity. First, the detection of spikes is enhanced in particular for low amplitude spikes, i.e. produced by mid-distant neurons. It might then be possible with such methods to broaden the vision of the micro-electrode by identifying the action potentials of neurons hidden by the noise, or for which the shapes are impossible to distinguish (known as Multi-Units (Quian Quiroga et al., 2004)).

We also illustrate that eliminating the propagated LFP clarifies the analysis of the local LFP, e.g. it reveals possible particular patterns appearing in the activity of the local structure with respect to a given stimuli. We expect that such separation will allow more accurate evaluation of the relationships between the detected spikes and the local LFP, but also possible relations with propagated distant LFP activities.

Separating the reference from the rest of the signal will also give the opportunity to study the inter-scale relations between the SEEG and the micro-electrodes. Indeed, due to its size, the potential as seen by the reference electrode may be comparable to the one of a macro SEEG electrode, and then might be considered as a macro sensor located within the implanted region. As a perspective, it will then be possible to separate the activity of the population from more distant structures by comparing the reference signal with the SEEG signal of the nearest contact, then splitting the LFP in three parts as the local LFP, the implanted population LFP, and the propagated LFP activity of distant structures.

This new separation method will be further evaluated on real data in acquisition related to FPVS stimulation (Rossion et al., 2015). This methodology is a promising tool for disentangling the responses of the targeted brain structure at different scales and will help in clarifying its involvement in the Human face recognition process.

ACKNOWLEDGEMENTS

REFERENCES

Buzsáki, G., Anastassiou, C. A., and Koch, C. (2012). The origin of extracellular fields and currents - EEG, ECoG, LFP and spikes. *Nature Reviews, Neuroscience*, 13:407–420.

Einevoll, G. T., Kayser, C., Logothetis, N. K., and Panzeri, S. (2013). Modelling and analysis of local field potentials for studying the function of cortical circuits. *Nat Rev Neurosci*, 14(11):770–785.

Eleftheriou, E. and Falconer, D. (1986). Tracking properties and steady-state performance of rls adaptive filter algorithms. *IEEE Transactions on Acoustics, Speech, and Signal Processing*, 34(5):1097–1110.

Hagen, E., Dahmen, D., Stavrinou, M. L., Lindén, H., Tetzlaff, T., van Albada, S. J., Grün, S., Diesmann, M., and Einevoll, G. T. (2016). Hybrid scheme for modeling local field potentials from point-neuron networks. *Cerebral Cortex*, 26(12):4461–4496.

Hjorth, B. (1975). An on-line transformation of EEG scalp potentials into orthogonal source derivations. *Electroencephalography and Clinical Neurophysiology*, 39(5):526 – 530.

Hofmanis, J., Caspary, O., Louis-Dorr, V., and Maillard, L. (2011). Automatic depth electrode localization in intracranial space. In *4th International Conference on Bio-inspired Systems and Signal Processing, Biosignals 2011*, Rome, Italie.

Hu, S., Stead, M., and Worrel, G. (2007). Automatic identification and removal of scalp reference signal for intracranial EEGs based on Independent Component Analysis. *IEEE Transactions on Biomedical Engineering*, 54(9):1560–1572.

Hu, S., Stead, M., and Worrell, G. (2008). Removal of scalp reference signal and line noise for intracranial EEGs. In *Networking, Sensing and Control, 2008. ICNSC 2008. IEEE International Conference on*, pages 1486–1491.

Kajikawa, Y. and Schroeder, C. E. (2011). How local is the local field potential? *Neuron*, (72).

Le Cam, S., Tran, H., Ranta, R., and Louis-Dorr, V. (2019). Simultaneous separation and sorting of extra-cellular spikes. In *9th International IEEE/EMBS Conference on Neural Engineering, NER 2019*, San Francisco, USA.

Libenson, M. (2012). *Practical approach to electroencephalography*. Elsevier Health Sciences.

Lindén, H., Pettersen, K. H., and Einevoll, G. T. (2010). Intrinsic dendritic filtering gives low-pass power spectra of local field potentials. *Journal of computational neuroscience*, 29(3):423–444.

Madhu, N., Ranta, R., Maillard, L., and Koessler, L. (2012). A unified treatment of the reference estimation problem in depth EEG recordings. *Med. Biol. Eng. Comput.*, 50(10):1003–1015.

Mitzdorf, U. (1985). Current source-density method and application in cat cerebral cortex: investigation of evoked potentials and EEG phenomena. *Physiological reviews*, 65(1):37–100.

Nelson, M. J., Pouget, P., Nilsen, E. A., Patten, C. D., and Schall, J. D. (2008). Review of signal distortion through metal microelectrode recording circuits and filters. *Journal of Neuroscience Methods*, 169:141–157.

Quian Quiroga, R., Nadasdy, Z., and Ben-Shaul, Y. (2004). Unsupervised spike detection and sorting with wavelets and superparamagnetic clustering. *Neural computation*, 16(8):1661–1687.

Ranta, R., Salido-Ruiz, R., and Louis-Dorr, V. (2010). Reference estimation in EEG recordings. In *32nd Ann. Int. Conf. of the IEEE-EMBS*, Buenos Aires, Argentina.

Rossion, B., Retter, T., and Liu-Shuang, J. (2020). Understanding human individuation of unfamiliar faces with oddball fast periodic visual stimulation and electroencephalography. *European Journal of Neuroscience (review)*.

Rossion, B., Torfs, K., Jacques, C., and Liu-Shuang, J. (2015). Fast periodic presentation of natural images reveals a robust face-selective electrophysiological response in the human brain. *Journal of Vision*, 15(1):18–18.

Salido-Ruiz, R. A., Ranta, R., Korats, G., Le Cam, S., Koessler, L., and Louis-Dorr, V. (2019). A unified weighted minimum norm solution for the reference inverse problem in eeg. *Computers in Biology and Medicine*, 115:103510.

Tran, H., Ranta, R., Le Cam, S., and Louis-Dorr, V. (2020). Fast simulation of extracellular action potential signatures based on a morphological filtering approximation. *Journal of Computational Neuroscience*, 48.

Yao, D. (2001). A method to standardize a reference of scalp EEG recordings to a point at infinity. *Physiological Measurement*, 22:693–711.

Zanos, T. P., Mineault, P. J., and Pack, C. C. (2011). Removal of spurious correlations between spikes and local field potentials. *J Neurophysiology*, 105:474–486.